Preprint typeset in JHEP style - HYPER VERSION

DO-TH 07/05
LPSC 07-29
SMU-HEP 07-07

Single pion electro– and neutrinoproduction on heavy targets

E. A. Paschos

Theoretische Physik III, University of Dortmund, D-44221 Dortmund, Germany
E-mail: paschos@physik.uni-dortmund.de

I. Schienbein

Laboratoire de Physique Subatomique et de Cosmologie,
Université Joseph Fourier/CNRS-IN2P3,
53 Avenue des Martyrs, F-38026 Grenoble, France
E-mail: schien@lpsc.in2p3.fr

J.-Y. Yu

Southern Methodist University, Dallas, Texas 75275, USA
E-mail: yu@physics.smu.edu

Abstract: We present a calculation of single pion electroproduction cross sections on heavy targets in the kinematic region of the $\Delta(1232)$ resonance. Final state interactions of the pions are taken into account using the pion multiple scattering model of Adler, Nussinov and Paschos (ANP model). For electroproduction and neutral current reactions we obtain results for carbon, oxygen, argon and iron targets and find a significant reduction of the W-spectra for π^0 as compared to the free nucleon case. On the other hand, the charged pion spectra are only little affected by final state interactions. Measurements of such cross sections with the CLAS detector at JLAB could help to improve our understanding of pion rescattering effects and serve as important/valuable input for calculations of single pion neutrinoproduction on heavy targets relevant for current and future long baseline neutrino experiments. Two ratios, in Eq. (3.8) and (3.10), will test important properties of the model.

Keywords: single pion production, nuclear effects, long baseline experiments.

Contents

1. Introduction

Neutrino interactions at low and medium energies are attracting attention because they will be measured accurately in the new generation of experiments [1, 2]. One aim of the experiments is to measure the precise form of the cross sections and their dependence on the input parameters. This way we check their couplings and compare the functional dependence of the form factors, where deviations from the dipole dependence have already been established (see e.g. figure 1 in [3] and references therein). Deviation from the standard model predictions can arise either from properties of the neutrinos or from new couplings of the gauge bosons to the particles in the target. Another aim of the experiments is to establish the properties of neutrinos including their masses, mixings and their fermionic nature (Dirac or Majorana particles). This program requires a good understanding of the cross sections, which motivated a new generation of calculations. Since the experiments use nuclear targets, like C^{12}, O^{16}, Ar^{40}, Fe^{56}, ... it is necessary to understand the modifications brought about by the targets.

The very old calculations for quasi-elastic scattering and resonance excitation on free nucleons [4, 5] have been replaced by new results where couplings and form factors are now better determined. For the vector couplings comparisons with electroproduction data have been very useful [3, 6]. Axial couplings are frequently determined by PCAC. There are already improvements and checks of the earlier quark models [7]. Comparisons with

experimental data are also available even though the experimental results are not always consistent with each other [8, 9, 10] but there are plans for improvements that will resolve the differences [1, 2].

For reactions on nuclear targets there are modifications brought about by the propagation of the produced particles in the nuclear medium. They involve absorption of particles, restrictions from Pauli blocking, Fermi motion and charge-exchange rescatterings. One group of papers uses nuclear potentials for the propagation of the particles [11]. Others use a transport theory of the final particles including channels coupled to each other [12]. These groups gained experience by analyzing reactions with electron beams (electroproduction) and adopted their methods to neutrino reactions [12].

Our group investigated 1-π pion production on medium and heavy targets employing the pion multiple scattering model by Adler, Nussinov and Paschos [13] that was developed in order to understand neutral current neutrino interactions with nuclei. This model was useful in the discovery of neutral currents and has been applied to predict neutrino-induced single pion production on Oxygen, Argon and Iron targets [14, 15, 16] which are used in long baseline(LBL) experiments. Among its characteristics is the importance of charge-exchange reactions that modify the $\pi^+ : \pi^0 : \pi^-$ ratios of the original neutrino-nucleon interaction through their scatterings within the nuclei. The presence of this effect has been confirmed by experiments [17]. We note here that our results are valid for isoscalar targets. For non-isoscalar targets like lead, used in the OPERA experiment, it is possible to extend the ANP model [18], which can be done in the future.

In this article we take an inverse route and use our calculation in neutrino reactions to go back to the electroproduction of pions on free nucleons and heavy nuclei. The plan of the paper is as follows. In section 2 we summarize the neutrino production cross sections on free nucleons and in the Δ resonance region. This topic has been described by several groups in the past few years. We present cross sections differential in several variables E_π, Q^2 and W. We pay special attention to the spectrum $d\sigma/dE_\pi$, where we correct an error we found in our earlier calculation [14]. Then we obtain the electroproduction cross section by setting the axial coupling equal to zero and rescaling, appropriately, the vector current contribution.

The main content of the article appears in section 3 where we describe the salient features and results of the ANP model. This model has the nice property that it can be written in analytic form including charge exchange and absorption of pions. This way we can trace the origin of the effects and formulate quantities which test specific terms and parameters. As we mentioned above several features have been tested already, and we wish to use electroproduction data in order to determine the accuracy of the predictions. We present numerical results for different target materials, and study the quality of the averaging approximation and uncertainties of the ANP model due to pion absorption effects. We discuss how the shape of the pion absorption cross section (per nucleon), an important and almost unconstrained ingredient of the ANP model, can be delineated from a measurement of the total fraction of absorbed pions. Finally, in Sec. 4 we summarize the main results. Averaged rescattering matrices for carbon, oxygen, argon, and iron targets and for different amounts of pion absorption have been collected in the appendices and are

useful for simple estimates of the rescattering effects.

2. Free nucleon cross sections

In the following sections, leptonic pion production on nuclear targets is regraded as a two step process. In the first step, the pions are produced from constituent nucleons in the target with free lepton-nucleon cross sections [13]. In the second step the produced pions undergo a nuclear interaction described by a transport matrix. Of course, the resonances themselves propagate in the nuclear medium before they decay, an effect that we will investigate in the future.

The leptonic production of pions in the Δ-resonance region is theoretically available and rather well understood as described in articles for both electro- and neutrino production, where comparisons with available data are in good agreement [3, 6, 7, 19, 12].

The available data is described accurately with the proposed parameterizations. The vector form factors are modified dipoles [3] which reproduce the helicity amplitudes measured in electroproduction experiments at Jefferson Laboratory [7]. The coupling in the axial form factors are determined by PCAC and data. Their functional dependence in Q^2 is determined by fitting the $\frac{\mathrm{d}\sigma}{\mathrm{d}Q^2}$ distributions. For the vector form factors the magnetic dipole dominance for $C_3^V(q^2)$ and $C_4^V(q^2)$ gives an accurate description of the data. However, deviations with a non-zero $C_5^V(q^2)$ have also been established [7]. This way a small (5%) isoscalar amplitude is reproduced.

For the propose of this article we shall use a scaling relation connecting neutrino- to electroproduction. The weak vector current is in the same isospin multiplied with the electromagnetic current and the two are related as follows:

$$< \Delta^{++}|V|p >= \sqrt{3} < \Delta^{+}|J_{em}^{I=1}|p >= \sqrt{3} < \Delta^{0}|J_{em}^{I=1}|n > \ .$$

Taking into account the isospin Clebsch-Gordan factors for the $\Delta \to N\pi$ branchings one finds the following contributions of the Δ-resonance to the cross sections for $ep \to ep\pi^0$, $ep \to en\pi^+$, $en \to ep\pi^-$ and $en \to en\pi^0$

$$\frac{\mathrm{d}\sigma^{em,I=1}}{\mathrm{d}Q^2\mathrm{d}W} = \frac{8}{3}\frac{\pi^2}{G_F^2}\frac{\alpha^2}{Q^4}\frac{\mathrm{d}V^\nu}{\mathrm{d}Q^2\mathrm{d}W} \times \begin{cases} \frac{2}{3} & : p\pi^0 \\ \frac{1}{3} & : n\pi^+ \\ \frac{1}{3} & : p\pi^- \\ \frac{2}{3} & : n\pi^0 \end{cases} \tag{2.1}$$

where $\frac{\mathrm{dV}^\nu}{\mathrm{dQ}^2\mathrm{dW}}$ denotes the cross section for the vector contribution alone to the reaction $\nu p \to \mu^- p\pi^+$. The free nucleon cross sections in Eq. (2.1) will be used in our numerical analysis. We shall call this the reduced electromagnetic formula. Its accuracy was tested in figure (5) of ref. [3]. Further comparisons can be found in [20].

For studies of the pion angular distributions (or what is the same of the pion energy spectrum in the laboratory frame) we begin with the triple differential cross section for

neutrino production

$$\frac{\mathrm{d}\sigma}{\mathrm{d}Q^2\mathrm{d}W\,\mathrm{d}\cos\theta_\pi^\star} = \frac{WG_F^2}{16\pi M_N^2}\sum_{i=1}^{3}\left(K_i\widetilde{W}_i - \frac{1}{2}K_iD_i(3\cos^2\theta_\pi^\star - 1)\right) \tag{2.2}$$

with K_i being kinematic factors of W and Q^2 and the structure functions $\widetilde{W}_i(Q^2, W)$ and $D_i(Q^2, W)$ representing the dynamics for the process. All of them are found in ref. [5]. The angle $\theta_\pi^\star$ is the polar angle of the pion in the CM frame with

$$\cos\theta_\pi^\star = \frac{-\gamma E_\pi^{\mathrm{CMS}} + E_\pi}{\beta\gamma|\vec{p}_\pi^{\,\mathrm{CMS}}|} \tag{2.3}$$

where

$$|\vec{p}_\pi^{\,\mathrm{CMS}}| = \sqrt{(E_\pi^{\mathrm{CMS}})^2 - m_\pi^2} \quad with \quad E_\pi^{\mathrm{CMS}} = \frac{W^2 + m_\pi^2 - M_N^2}{2W} \tag{2.4}$$

and the rest of the variables defined as

$$\nu = \frac{W^2 + Q^2 - M_N^2}{2M_N}\,,\ \gamma = \frac{\nu + M_N}{W}\,,\ \beta\gamma = \frac{\sqrt{\nu^2 + Q^2}}{W}. \tag{2.5}$$

It is now straight-forward to convert the cross section differential in the solid angle to the one differential in the laboratory energy of the pion, E_π,

$$\frac{d\sigma}{dE_\pi} = \frac{1}{\gamma\beta|\vec{p}_\pi^{\,\mathrm{CMS}}|}\frac{d\sigma}{d\cos\theta_\pi^\star}\,. \tag{2.6}$$

Having expressed all quantities in (2.2) and (2.5) in terms of W, Q^2 and E_π it is possible to compute the pion energy spectrum

$$\frac{d\sigma}{dE_\pi} = \int_{W_{\min}}^{W_{\max}} dW \int_{Q^2_{\min}}^{Q^2_{\max}} dQ^2\ \frac{d\sigma}{dQ^2 dW dE_\pi}\ \theta(phys). \tag{2.7}$$

The limits of integration are given as

$$\begin{aligned} Q^2_{\min} &= 0\,, \quad Q^2_{\max} = \frac{(S - W^2)(S - M_N^2)}{S}, \\ W_{\min} &= M_N + m_\pi\,, \quad W_{\max} \simeq 1.6\ \mathrm{GeV} \end{aligned} \tag{2.8}$$

where $S = M_N^2 + 2M_NE_1$ is the center-of-mass energy squared with E_1 the energy of the incoming lepton in the LAB system. The θ-function takes care of the constraints from the phase space. We integrated the cross section for $E_\nu = 1$ GeV and show the spectrum in figures 1–3. In our earlier publication [14] the spectrum for E_π was incorrect because we did not impose the phase space constraints correctly. The pion spectrum for charged current reactions is correctly reported in figure (4) in ref. [21]. The discrepancy in ref. [14] has been pointed out for neutral currents in ref [12].

The neutrino–nucleon and electron–nucleon cross sections will be used in the rest of this article in order to compute and test effects of nuclear corrections. We deduce the electroproduction cross sections from neutrino production as in Eq. (2.1). For the triple

differential cross section we follow the same procedure by setting the axial form factors to zero and using the relation

$$\frac{\mathrm{d}\sigma^{em,I=1}}{\mathrm{d}Q^2\mathrm{d}W\mathrm{d}E_\pi} = \frac{8}{3}\frac{\pi^2}{G_F^2}\frac{\alpha^2}{Q^4}\frac{\mathrm{d}V^\nu}{\mathrm{d}Q^2\mathrm{d}W\mathrm{d}E_\pi} \times \begin{cases} \frac{2}{3} & : ep \to ep\pi^0 \\ \frac{1}{3} & : ep \to en\pi^+ \\ \frac{1}{3} & : en \to ep\pi^- \\ \frac{2}{3} & : en \to en\pi^0 \end{cases} \tag{2.9}$$

A small isoscalar part in the electromagnetic cross section is omitted since it does not contribute to the Δ-resonance but only to the background, which for $W < 1.3$ GeV is small and contributes for 1.3 GeV $< W <$ 1.4 GeV.

3. Cross sections for heavy targets

In the following we will deal with single pion resonance production in the scattering of a lepton l off a nuclear target T ($_6C^{12}$, $_8O^{16}$, $_{18}Ar^{40}$, $_{26}Fe^{56}$), i.e., with the reactions

$$l + T \to l' + T' + \pi^{\pm,0} \tag{3.1}$$

where l' is the outgoing lepton and T' a final nuclear state. Furthermore, in our analysis of nuclear rescattering effects we will restrict ourselves to the region of the $\Delta(1232)$ resonance, 1.1 GeV $< W <$ 1.4 GeV, and to isoscalar targets with equal number of protons and neutrons.

3.1 Pion rescattering in the ANP model

According to the ANP model [13, 22] the final cross sections for pions $(\pi^+, \pi^0, \pi^-)_f$ can be related to the initial cross sections $(\pi^+, \pi^0, \pi^-)_i$ for a *free nucleon* target in the simple form

$$\begin{pmatrix} \frac{\mathrm{d}\sigma(_ZT^A;\pi^+)}{\mathrm{d}Q^2\mathrm{d}W} \\ \frac{\mathrm{d}\sigma(_ZT^A;\pi^0)}{\mathrm{d}Q^2\mathrm{d}W} \\ \frac{\mathrm{d}\sigma(_ZT^A;\pi^-)}{\mathrm{d}Q^2\mathrm{d}W} \end{pmatrix}_{\mathrm{f}} = M[T;Q^2,W] \begin{pmatrix} \frac{\mathrm{d}\sigma(N_T;\pi^+)}{\mathrm{d}Q^2\mathrm{d}W} \\ \frac{\mathrm{d}\sigma(N_T;\pi^0)}{\mathrm{d}Q^2\mathrm{d}W} \\ \frac{\mathrm{d}\sigma(N_T;\pi^-)}{\mathrm{d}Q^2\mathrm{d}W} \end{pmatrix}_{\mathrm{i}} \tag{3.2}$$

with

$$\frac{\mathrm{d}\sigma(N_T;\pm 0)}{\mathrm{d}Q^2\mathrm{d}W} = Z\frac{\mathrm{d}\sigma(p;\pm 0)}{\mathrm{d}Q^2\mathrm{d}W} + (A-Z)\frac{\mathrm{d}\sigma(n;\pm 0)}{\mathrm{d}Q^2\mathrm{d}W} \tag{3.3}$$

where the free nucleon cross sections are averaged over the Fermi momentum of the nucleons.[1] For an isoscalar target the matrix M is described by three independent parameters A_p, d, and c in the following form [13]

$$M = A_p \begin{pmatrix} 1-c-d & d & c \\ d & 1-2d & d \\ c & d & 1-c-d \end{pmatrix} , \tag{3.4}$$

[1] However, the Fermi motion has a very small effect on the W distribution and we neglect it in our numerical analysis. On the other hand, effects of the Pauli exclusion principle have been absorbed into the matrix M and are taken into account.

where $A_p(Q^2,W) = g(Q^2,W) \times f(1,W)$. Here, $g(Q^2,W)$ is the Pauli suppression factor and $f(1,W)$ is a transport function for equal populations of π^+,π^0,π^- which depends on the absorption cross section of pions in the nucleus. The parameters c and d describe the charge exchange contribution. The final yields of π's depend on the target material and the final state kinematic variables, i.e., $M = M[T;Q^2,W]$.

In order to simplify the problem it is helpful to integrate the doubly differential cross sections of Eq. (3.2) over W in the $(3,3)$ resonance region, say, $m_p + m_\pi \leq W \leq 1.4$ GeV. In this case Eq. (3.2) can be replaced by an equation of identical form

$$\begin{pmatrix} \frac{\mathrm{d}\sigma({}_Z T^A;\pi^+)}{\mathrm{d}Q^2} \\ \frac{\mathrm{d}\sigma({}_Z T^A;\pi^0)}{\mathrm{d}Q^2} \\ \frac{\mathrm{d}\sigma({}_Z T^A;\pi^-)}{\mathrm{d}Q^2} \end{pmatrix}_{\mathrm{f}} = \overline{M}[T;Q^2] \begin{pmatrix} \frac{\mathrm{d}\sigma(N_T;\pi^+)}{\mathrm{d}Q^2} \\ \frac{\mathrm{d}\sigma(N_T;\pi^0)}{\mathrm{d}Q^2} \\ \frac{\mathrm{d}\sigma(N_T;\pi^-)}{\mathrm{d}Q^2} \end{pmatrix}_{\mathrm{i}} \tag{3.5}$$

where the matrix $\overline{M}[T;Q^2]$ can be obtained by averaging the matrix $M[T;Q^2,W]$ over W with the leading W-dependence coming from the Δ resonance contribution. Moreover, we expect the matrix M to be a slowly varying function of Q^2 (for $Q^2 \gtrsim 0.3$ GeV^2). For this reason we introduce a second averaging over Q^2 and define the double averaged matrix $\overline{\overline{M}}[T]$ which is particularly useful for giving a simple description of charge exchange effects in different nuclear targets. In the double-averaging approximation (AV2) the final cross sections including nuclear corrections are expressed as follows:

$$\begin{pmatrix} \frac{\mathrm{d}\sigma({}_Z T^A;\pi^+)}{\mathrm{d}Q^2\mathrm{d}W} \\ \frac{\mathrm{d}\sigma({}_Z T^A;\pi^0)}{\mathrm{d}Q^2\mathrm{d}W} \\ \frac{\mathrm{d}\sigma({}_Z T^A;\pi^-)}{\mathrm{d}Q^2\mathrm{d}W} \end{pmatrix}_{\mathrm{f}} = \overline{\overline{M}}[T] \begin{pmatrix} \frac{\mathrm{d}\sigma(N_T;\pi^+)}{\mathrm{d}Q^2\mathrm{d}W} \\ \frac{\mathrm{d}\sigma(N_T;\pi^0)}{\mathrm{d}Q^2\mathrm{d}W} \\ \frac{\mathrm{d}\sigma(N_T;\pi^-)}{\mathrm{d}Q^2\mathrm{d}W} \end{pmatrix}_{\mathrm{i}} . \tag{3.6}$$

We note that the cross sections are differential in two variables while the matrix $\overline{\overline{M}}[T]$ is the average over these variables.

The above discussion will be used for a phenomenological description of nuclear rescattering effects. On the other hand, in Ref. [13] a dynamical model has been developed to calculate the charge exchange matrix M. As an example, for oxygen the resulting matrix in the double-averaging approximation is given by

$$\overline{\overline{M}}({}_8O^{16}) = \overline{\overline{A_p}} \begin{pmatrix} 0.788 & 0.158 & 0.0537 \\ 0.158 & 0.684 & 0.158 \\ 0.0537 & 0.158 & 0.788 \end{pmatrix} . \tag{3.7}$$

with $\overline{\overline{A_p}} = 0.766$, which contains the averaged Pauli suppression factor and absorption of pions in the nucleus. There are various absorption models described in the original article. Two of them are distinguished by the energy dependence of the absorption cross section beyond the Δ region. In model [A] the absorption increases as W increases while in [B]

it decreases for large W's (beyond the Δ region). A comparison of the two absorption models (A) and (B) can be found in [22]. Since the fraction of absorbed pions is still rather uncertain we provide in the appendices ANP matrices for different amounts of absorption. These matrices are useful to obtain an uncertainty band for the expected nuclear corrections.

3.2 Results for various targets

In this section we present numerical results for 1-pion leptoproduction differential cross sections including nuclear corrections using the ANP model outlined in the preceding section.

3.2.1 Neutrinoproduction

We begin with a discussion of the nuclear corrections to the pion energy spectra in neutrino scattering shown in Figs. 1–3, where the curves are neutral current reactions. The dotted lines are the spectra for the free nucleon cross sections. The dashed lines include the effect of the Pauli suppression (in step one of the two step process), whereas the solid line in addition takes into account the pion multiple scattering. These curves correct Figs. 8–16 in Ref. [14]. Similar curves have been obtained recently by Leitner et al. [12] who also noticed the error in [14]. Even though the models differ in the transport matrix, they both include charge exchange effects. For example, they both find that for reactions where the charge of the pions is the same with the charge of the current the pion yield shows a substantial decrease.

3.2.2 Electroproduction

We now turn to the electroproduction. To be specific, our analysis will be done under the conditions of the Cebaf Large Acceptance Spectrometer (CLAS) at Jefferson Lab (JLAB). The CLAS detector [23] covers a large fraction of the full solid angle with efficient neutral and charged particle detection. Therefore it is very well suited to perform a high statistics measurement on various light and heavy nuclear targets and to test the ideas of pion multiple scattering models. In the future these measurements can be compared with results in neutrinoproduction from the Minerva experiment [1] using the high intensity Numi neutrino beam. If not stated otherwise we use an electron energy $E_e = 2.7$ GeV in order to come as close as possible to the relevant low energy range of the LBL experiments. For the momentum transfer we take the values $Q^2 = 0.4, 0.8$ GeV^2 in order to avoid the experimentally and theoretically more problematic region at very low Q^2. Results for larger Q^2 and larger energies, say $E_e = 10$ GeV, are qualitatively very similar.

Figure 4 shows the double differential cross section $\mathrm{d}\sigma/\mathrm{d}Q^2\mathrm{d}W$ for π^+ and π^0 production versus W for an oxygen target. The solid lines have been obtained with help of Eq. (3.2) including the nuclear corrections. The dashed lines show the result of the double-averaging approximation according to Eq. (3.6) using the ANP matrix in Eq. (3.7). The dotted line is the free cross section in Eq. (3.3). One sees, the double-averaging approximation and the exact calculation give very similar results such that the former is well-suited for simple estimates to an accuracy of 10% of pion rescattering effects. We observe that

the cross sections for π^0 production are largely reduced by about 40% due to the nuclear corrections. This can be understood since the larger π^0 cross sections are reduced by absorption effects and charge exchange effects. On the other hand, the π^+ cross sections are even slightly enlarged, because the reduction due to pion absorption is compensated by an increase due to charge exchange. The compensation is substantial since the π^0 yields are dominant.

In Fig. 5 double differential cross sections per nucleon for different target materials are presented. The electron energy and the momentum transfer have been chosen as $E_e = 2.7$ GeV and $Q^2 = 0.4$ GeV^2, respectively. The results for the pion rescattering corrections have been obtained within the double-averaging approximation (3.6) which allows for a simple comparison of the dependence on the target material in terms of the matrices $\overline{\overline{M}}[T]$ which can be found in Eq. (3.7) and App. A. For comparison the free nucleon cross section (3.3) (isoscalar $\frac{p+n}{2}$) is also shown. As expected, the nuclear corrections become larger with increasing atomic number from carbon to iron.

One of the input quantities for calculating the transport function $f(\lambda)$ in the ANP model is the pion absorption cross section $\sigma_{\rm abs}(W)$ describing the probability that the pion is absorbed in a single rescattering process. For $\sigma_{\rm abs}(W)$ the ANP article reported results for two parameterizations, models A and B, taken from Refs. [24, 25] which have very different W-dependence and normalization. However, the predictions of the ANP model in the double-averaging approximation are primarily sensitive to the normalization of the pion absorption cross section at $W \simeq m_\Delta$ [22]. Using data by Merenyi et al. [26] for a neon target it was found that about $25\% \pm 5\%$ of pions are absorbed making possible the determination of the normalization of $\sigma_{\rm abs}(W)$ with a 20% accuracy.

In order to investigate the theoretical uncertainty due to pion absorption effects we show in Fig. 6 double differential cross sections $\mathrm{d}\sigma/\mathrm{d}Q^2\mathrm{d}W$ for π^+ and π^0 production vs W for different amounts of pion absorption in oxygen: 25% (solid line), 20% (dashed line), 30% (dotted line). The π^0 and π^+ spectra have been calculated in the double-averaging approximation (3.6) utilizing the matrices in App. B. The three curves represent the theoretical uncertainty due to pion absorption effects. For comparison, the free nucleon cross section (3.3) is shown as well.

Although the predictions of the ANP model are mainly sensitive to $\sigma_{\rm abs}(W \simeq m_\Delta)$ it would be interesting to obtain more information on the detailed W-shape. The fraction of absorbed pions can be determined by measuring the inclusive pion production cross sections for a nuclear target divided by the free nucleon cross sections,

$$\mathrm{Abs(Q^2,W)} = 1 - \frac{\sum_{\mathrm{k}=0,\pm} \frac{\mathrm{d}\sigma(_{\mathrm{Z}}\mathrm{T}^{\mathrm{A}};\pi^{\mathrm{k}})}{\mathrm{dQ^2dW}}}{\sum_{\mathrm{j}=0,\pm} \frac{\mathrm{d}\sigma(\mathrm{N_T};\pi^{\mathrm{j}})}{\mathrm{dQ^2dW}}} = 1 - \mathrm{A_p(Q^2,W)}\,, \tag{3.8}$$

where A_p has been introduced in (3.4). This quantity is related to $\sigma_{\rm abs}(W)$ as can be seen by linearizing the transport function $f(\lambda, W)$ [16, 22]

$$\mathrm{Abs(Q^2,W)} \simeq \frac{1}{2}\bar{\mathrm{L}}\rho_0 \times \sigma_{\rm abs}(\mathrm{W})\ . \tag{3.9}$$

Here $\bar{L}$ is the effective length of the nucleus averaged over impact parameters and ρ_0 the charge density in the center. As an example, for oxygen one finds $\bar{L} \simeq 1.9R$ with radius $R \simeq 1.833$ fm and $\rho_0 = 0.141$ fm^{-3}. Therefore, the W-dependence of $\sigma_{\rm abs}(W)$ can be reconstructed from the fraction of absorbed pions, i.e. Abs(Q^2, W). Summing over the three charged pions eliminates charge exchange effects.

In order to verify the linearized approximation in Eq. (3.9), we show in Fig. 7 the ANP model prediction for Abs(Q^2, W) for oxygen and iron targets with $Q^2 = 0.3$ GeV^2. This prediction strongly depends on the shape of the cross section $\sigma_{\rm abs}(W)$ for which we use model B from Refs. [25]. $\sigma_{\rm abs}(W)$ multiplied by a free normalization factors for oxygen and iron, respectively, is depicted by the dashed lines. Obviously, Eq. (3.9) is quite well satisfied for oxygen and still reasonably good for iron. Finally, the dotted line shows the result of the averaging approximation. We conclude that $\sigma_{\rm abs}(W)$ can be extracted with help of Eqs. (3.8) and (3.9).

For completeness, we mention that the pion absorption in nuclei is reported in various articles [27]. For comparisons one should be careful because the absorption cross sections in pi-nucleus and in neutrino-nucleus reactions are different, in the former case it is a surface effect while in the latter it occurs everywhere in the nucleus.

A useful test of charge exchange effects is provided by the double ratio

$$\mathrm{DR}(Q^2, W) = \left(\frac{\pi^0}{\pi^+ + \pi^-}\right)_A \Big/ \left(\frac{\pi^0}{\pi^+ + \pi^-}\right)_p \tag{3.10}$$

where $(\pi^i)_A$ represents the doubly differential cross section $\mathrm{d}\sigma/\mathrm{d}Q^2\mathrm{d}W$ for the production of a pion π^i in eA scattering. This observable is expected to be rather robust with respect to radiative corrections and acceptance differences between neutral and charged pions.[2] In Fig. 8 we show the double ratio for a carbon target in dependence of W for a fixed $Q^2 = 0.4$ GeV^2. The dependence on Q^2 is weak and results for other values of Q^2 are very similar. The solid line shows the exact result, whereas the dotted lines have been obtained in the double averaging approximation with minimal and maximal amounts of pion absorption. As can be seen, the results are rather insensitive to the exact amount of pion absorption. Without charge exchange effects (and assuming similar absorption of charged and neutral pions) the double ratio would be close to unity. As can be seen, the ANP model predicts a double ratio smaller than 0.6 in the region $W \simeq 1.2$ GeV. A confirmation of this expectation would be a clear signal of pion charge exchange predominantly governed by isospin symmetry. In this case it would be interesting to go a step further and to study similar ratios for pion angular distributions.

4. Summary

Lepton induced reactions on medium and heavy nuclei include the rescattering of produced pions inside the nuclei. This is especially noticeable in the Δ-resonance region, where the produced resonance decays into a nucleon and a pion. In the introduction and section

[2] We are grateful to S. Manly for drawing our attention to the double ratio.

2 we reviewed the progress that has been made in the calculations of neutrino-induced reactions on free protons and neutrons, because we needed them for following calculations. For several resonances the vector form factors have been recently determined by using electroproduction results in Jefferson Laboratory [7]. For the axial form factors modified dipoles give an accurate description of the data. For the purposes of this article (studies of nuclear corrections) it suffices to deduce the electroproduction cross sections through Eqs. (2.1) and (2.9).

The main contribution of this article is contained in section 3, where we describe important features of the ANP model and define single- and double averaged transport matrices. Two important aspects of rescattering are emphasized: (i) the absorption of the pions and (ii) charge exchange occurring in the multiple scattering, where we have shown that special features of the data are attributed to each of them. Finally we propose specific ratios of electroproduction reactions that are sensitive to the absorption cross section and to charge exchange effects.

Using the model we calculate the transport matrix for various absorption cross sections and nuclei and present the results in appendix A. We also calculated the pion energy spectra with and without nuclear corrections. The results appear in figures 1–3 and can be compared with other calculations [12]. Comparison of the double averaged approximation with the exact ANP calculation shows small differences (figure 4). As mentioned already, electroproduction data are very useful in testing several aspects of the model and its predictions. For the absorption cross section we propose in Eq. (3.8) a ratio that depends only on $\mathrm{A_p}(Q^2, W) = g(Q^2, W) f(1, W)$. Since we consider isoscalar targets and sum over the charges of the pions, charge exchange terms are eliminated. This leaves over the dependence on charge independent effects, like the Pauli factor and the average absorption; this is indeed the average absorption of pions and even includes the absorption of the Δ-resonance itself.

Another ratio ($\mathrm{DR}(Q^2, W)$) is sensitive to charge exchange effects. In the double ratio the dependence on $\mathrm{A_p}(Q^2, W)$ drops out and the surviving terms are isospin dependent. Our calculation shows that the ratio depends on W with the largest reduction occurring in the region $1.1 < W < 1.25$ GeV. Finally, the $\Delta(1232)$ is a sharply peaked resonance, where the resonant interaction, takes place over small ranges of the kinematic variables, so that averaging over them gives accurate approximations. This is analogous to a narrow width approximation. Several comparisons in this article confirm the expectation that averaged quantities give rather accurate approximations of more extensive calculations.

Acknowledgments

We wish to thank W. Brooks and S. Manly for many useful discussions, their interest and encouragement. The work of J. Y. Yu is supported by the Deutsche Forschungsgemeinschaft (DFG) through Grant No. YU 118/1-1.

Appendix

A. Charge exchange matrices in the double averaging approximation

Carbon:

$$\overline{\overline{M}}({}_6C^{12}) = \overline{\overline{A_p}} \begin{pmatrix} 0.826 & 0.136 & 0.038 \\ 0.136 & 0.728 & 0.136 \\ 0.038 & 0.136 & 0.826 \end{pmatrix} \tag{A.1}$$

with $\overline{\overline{A_p}} = 0.791$.

Argon:

$$\overline{\overline{M}}({}_{18}Ar^{40}) = \overline{\overline{A_p}} \begin{pmatrix} 0.733 & 0.187 & 0.080 \\ 0.187 & 0.626 & 0.187 \\ 0.080 & 0.187 & 0.733 \end{pmatrix} \tag{A.2}$$

with $\overline{\overline{A_p}} = 0.657$.
Iron:

$$\overline{\overline{M}}({}_{26}Fe^{56}) = \overline{\overline{A_p}} \begin{pmatrix} 0.720 & 0.194 & 0.086 \\ 0.194 & 0.613 & 0.194 \\ 0.086 & 0.194 & 0.720 \end{pmatrix} \tag{A.3}$$

with $\overline{\overline{A_p}} = 0.631$.

B. Charge exchange matrices for various amounts of pion absorption

Carbon:

15% absorption

$$\overline{\overline{M}}({}_6O^{12}) = \overline{\overline{A_p}} \begin{pmatrix} 0.817 & 0.141 & 0.041 \\ 0.141 & 0.718 & 0.141 \\ 0.041 & 0.141 & 0.817 \end{pmatrix} \tag{B.1}$$

with $\overline{\overline{A_p}} = 0.831$.

20% absorption

$$\overline{\overline{M}}({}_6C^{12}) = \overline{\overline{A_p}} \begin{pmatrix} 0.829 & 0.134 & 0.037 \\ 0.134 & 0.731 & 0.134 \\ 0.037 & 0.134 & 0.829 \end{pmatrix} \tag{B.2}$$

with $\overline{\overline{A_p}} = 0.782$.

25% absorption

$$\overline{\overline{M}}({}_6C^{12}) = \overline{\overline{A_p}} \begin{pmatrix} 0.840 & 0.127 & 0.032 \\ 0.127 & 0.745 & 0.127 \\ 0.032 & 0.127 & 0.840 \end{pmatrix} \tag{B.3}$$

with $\overline{\overline{A_p}} = 0.734$.

Oxygen:

15% absorption

$$\overline{\overline{M}}({}_8O^{16}) = \overline{\overline{A_p}} \begin{pmatrix} 0.771 & 0.167 & 0.062 \\ 0.167 & 0.665 & 0.167 \\ 0.062 & 0.167 & 0.771 \end{pmatrix} \tag{B.4}$$

with $\overline{\overline{A_p}} = 0.833$.

20% absorption

$$\overline{\overline{M}}({}_8O^{16}) = \overline{\overline{A_p}} \begin{pmatrix} 0.783 & 0.161 & 0.056 \\ 0.161 & 0.679 & 0.161 \\ 0.056 & 0.161 & 0.783 \end{pmatrix} \tag{B.5}$$

with $\overline{\overline{A_p}} = 0.784$.

25% absorption

$$\overline{\overline{M}}({}_8O^{16}) = \overline{\overline{A_p}} \begin{pmatrix} 0.797 & 0.153 & 0.050 \\ 0.153 & 0.693 & 0.153 \\ 0.050 & 0.153 & 0.797 \end{pmatrix} \tag{B.6}$$

with $\overline{\overline{A_p}} = 0.735$.

30% absorption

$$\overline{\overline{M}}({}_8O^{16}) = \overline{\overline{A_p}} \begin{pmatrix} 0.810 & 0.146 & 0.044 \\ 0.146 & 0.709 & 0.146 \\ 0.044 & 0.146 & 0.810 \end{pmatrix} \tag{B.7}$$

with $\overline{\overline{A_p}} = 0.687$.

C. Forward- and backward charge exchange matrices

Carbon:
15% absorption

$$\overline{\overline{M}}_+({}_6C^{12}) = \overline{\overline{A_{p+}}} \begin{pmatrix} 0.870 & 0.100 & 0.029 \\ 0.100 & 0.799 & 0.100 \\ 0.029 & 0.100 & 0.870 \end{pmatrix}, \overline{\overline{M}}_-({}_6C^{12}) = \overline{\overline{A_{p-}}} \begin{pmatrix} 0.675 & 0.251 & 0.074 \\ 0.251 & 0.498 & 0.251 \\ 0.074 & 0.251 & 0.675 \end{pmatrix} \tag{C.1}$$

with $\overline{\overline{A_{p+}}} = 0.606$ and $\overline{\overline{A_{p-}}} = 0.225$.

20% absorption

$$\overline{\overline{M}}_+({}_6C^{12}) = \overline{\overline{A_{p+}}} \begin{pmatrix} 0.880 & 0.094 & 0.026 \\ 0.094 & 0.811 & 0.094 \\ 0.026 & 0.094 & 0.880 \end{pmatrix}, \overline{\overline{M}}_-({}_6C^{12}) = \overline{\overline{A_{p-}}} \begin{pmatrix} 0.685 & 0.247 & 0.068 \\ 0.247 & 0.505 & 0.247 \\ 0.068 & 0.247 & 0.685 \end{pmatrix} \quad \text{(C.2)}$$

with $\overline{\overline{A_{p+}}} = 0.578$ and $\overline{\overline{A_{p-}}} = 0.204$.

25% absorption

$$\overline{\overline{M}}_+({}_6C^{12}) = \overline{\overline{A_{p+}}} \begin{pmatrix} 0.889 & 0.088 & 0.022 \\ 0.088 & 0.823 & 0.088 \\ 0.022 & 0.088 & 0.889 \end{pmatrix}, \overline{\overline{M}}_-({}_6C^{12}) = \overline{\overline{A_{p-}}} \begin{pmatrix} 0.695 & 0.243 & 0.062 \\ 0.243 & 0.513 & 0.243 \\ 0.062 & 0.243 & 0.695 \end{pmatrix} \quad \text{(C.3)}$$

with $\overline{\overline{A_{p+}}} = 0.549$ and $\overline{\overline{A_{p-}}} = 0.184$.

Oxygen:

15% absorption

$$\overline{\overline{M}}_+({}_8O^{16}) = \overline{\overline{A_{p+}}} \begin{pmatrix} 0.829 & 0.125 & 0.046 \\ 0.125 & 0.750 & 0.125 \\ 0.046 & 0.125 & 0.829 \end{pmatrix}, \overline{\overline{M}}_-({}_8O^{16}) = \overline{\overline{A_{p-}}} \begin{pmatrix} 0.635 & 0.265 & 0.100 \\ 0.265 & 0.470 & 0.265 \\ 0.100 & 0.265 & 0.635 \end{pmatrix} \quad \text{(C.4)}$$

with $\overline{\overline{A_{p+}}} = 0.581$ and $\overline{\overline{A_{p-}}} = 0.252$.

20% absorption

$$\overline{\overline{M}}_+({}_8O^{16}) = \overline{\overline{A_{p+}}} \begin{pmatrix} 0.840 & 0.119 & 0.041 \\ 0.119 & 0.762 & 0.119 \\ 0.041 & 0.119 & 0.840 \end{pmatrix}, \overline{\overline{M}}_-({}_8O^{16}) = \overline{\overline{A_{p-}}} \begin{pmatrix} 0.646 & 0.262 & 0.092 \\ 0.262 & 0.477 & 0.262 \\ 0.092 & 0.262 & 0.646 \end{pmatrix} \quad \text{(C.5)}$$

with $\overline{\overline{A_{p+}}} = 0.554$ and $\overline{\overline{A_{p-}}} = 0.23$.

25% absorption

$$\overline{\overline{M}}_+({}_8O^{16}) = \overline{\overline{A_{p+}}} \begin{pmatrix} 0.852 & 0.112 & 0.036 \\ 0.112 & 0.776 & 0.112 \\ 0.036 & 0.112 & 0.852 \end{pmatrix}, \overline{\overline{M}}_-({}_8O^{16}) = \overline{\overline{A_{p-}}} \begin{pmatrix} 0.657 & 0.258 & 0.085 \\ 0.258 & 0.485 & 0.257 \\ 0.085 & 0.258 & 0.657 \end{pmatrix} \quad \text{(C.6)}$$

with $\overline{\overline{A_{p+}}} = 0.527$ and $\overline{\overline{A_{p-}}} = 0.208$.

30% absorption

$$\overline{\overline{M}}_+({}_8O^{16}) = \overline{\overline{A_{p+}}} \begin{pmatrix} 0.863 & 0.105 & 0.031 \\ 0.105 & 0.789 & 0.105 \\ 0.031 & 0.105 & 0.863 \end{pmatrix}, \overline{\overline{M}}_-({}_8O^{16}) = \overline{\overline{A_{p-}}} \begin{pmatrix} 0.669 & 0.253 & 0.078 \\ 0.253 & 0.493 & 0.253 \\ 0.078 & 0.253 & 0.669 \end{pmatrix} \quad \text{(C.7)}$$

with $\overline{\overline{A_{p+}}} = 0.499$ and $\overline{\overline{A_{p-}}} = 0.187$.

References

[1] D. Drakoulakos *et al.*, Minerνa Collaboration (2004), hep-ex/0405002.

[2] K. B. M. Mahn, Nucl. Phys. Proc. Suppl. **159**, 237 (2006).
H. Gallagher, Nucl. Phys. Proc. Suppl. **159**, 229 (2006).
G. Giacomelli and M. Giorgini, OPERA Collaboration (2006), physics/0609045.

[3] E. A. Paschos, J.-Y. Yu, and M. Sakuda, Phys. Rev. **D69**, 014013 (2004), hep-ph/0308130.

[4] D. Rein and L. M. Sehgal, Ann. Phys. **133**, 79 (1981).

[5] P. A. Schreiner and F. Von Hippel, Nucl. Phys. **B58**, 333 (1973).

[6] O. Lalakulich and E. A. Paschos, Phys. Rev. **D71**, 074003 (2005), hep-ph/0501109.
T. Sato, D. Uno, and T. S. H. Lee, Phys. Rev. **C67**, 065201 (2003), nucl-th/0303050.

[7] O. Lalakulich, E. A. Paschos, and G. Piranishvili, Phys. Rev. **D74**, 014009 (2006), hep-ph/0602210.

[8] H. J. Grabosch *et al.*, SKAT Collaboration, Z. Phys. **C41**, 527 (1989).

[9] S. J. Barish *et al.*, Phys. Rev. **D19**, 2521 (1979).
G. M. Radecky *et al.*, Phys. Rev. **D25**, 1161 (1982), Erratum: **D26**, 3297 (1982).

[10] T. Kitagaki *et al.*, Phys. Rev. **D34**, 2554 (1986).

[11] L. Alvarez-Ruso, M. B. Barbaro, T. W. Donnelly, and A. Molinari, Nucl. Phys. **A724**, 157 (2003), nucl-th/0303027.

[12] T. Leitner, L. Alvarez-Ruso, and U. Mosel, Phys. Rev. **C74**, 065502 (2006), nucl-th/0606058.

[13] S. L. Adler, S. Nussinov, and E. A. Paschos, Phys. Rev. **D9**, 2125 (1974).

[14] E. A. Paschos, L. Pasquali, and J. Y. Yu, Nucl. Phys. **B588**, 263 (2000), hep-ph/0005255.

[15] E. A. Paschos and J. Y. Yu, Phys. Rev. **D65**, 033002 (2002), hep-ph/0107261.

[16] E. A. Paschos, I. Schienbein, and J. Y. Yu, Nucl. Phys. Proc. Suppl. **139**, 119 (2005), hep-ph/0408148.

[17] P. Musset and J. P. Vialle, Phys. Rept. **39**, 1 (1978), see section (3.7.5).

[18] S. L. Adler, Phys. Rev. **D9**, 2144 (1974).

[19] L. Alvarez-Ruso, S. K. Singh, and M. J. Vicente Vacas, Phys. Rev. **C59**, 3386 (1999), nucl-th/9804007.

[20] E. A. Paschos, M. Sakuda, I. Schienbein, and J. Y. Yu, Nucl. Phys. Proc. Suppl. **139**, 125 (2005), hep-ph/0408185.

[21] E. A. Paschos, D. P. Roy, I. Schienbein, and J. Y. Yu, Phys. Lett. **B574**, 232 (2003), hep-ph/0307223.

[22] I. Schienbein and J.-Y. Yu, talk presented at the *Second International Workshop on Neutrino-Nucleus Interactions in the few-GeV Region (NUINT'02)*, Irvine, California, December 2002. Homepage: http://www.ps.uci.edu/∼nuint/ , hep-ph/0308010.

[23] B. A. Mecking *et al.*, CLAS Collaboration, Nucl. Instrum. Meth. **A503**, 513 (2003).

[24] M. M. Sternheim and R. R. Silbar, Phys. Rev. **D6**, 3117 (1972).

[25] R. R. Silbar and M. M. Sternheim, Phys. Rev. **C8**, 492 (1973).

[26] R. Merenyi *et al.*, Phys. Rev. **D45**, 743 (1992).

[27] D. Ashery and J. P. Schiffer, Ann. Rev. Nucl. Part. Sci. **36**, 207 (1986).
C. H. Q. Ingram, Nucl. Phys. **A684**, 122 (2001).
R. D. Ransome, Nucl. Phys. Proc. Suppl. **139**, 208 (2005), and references therein.

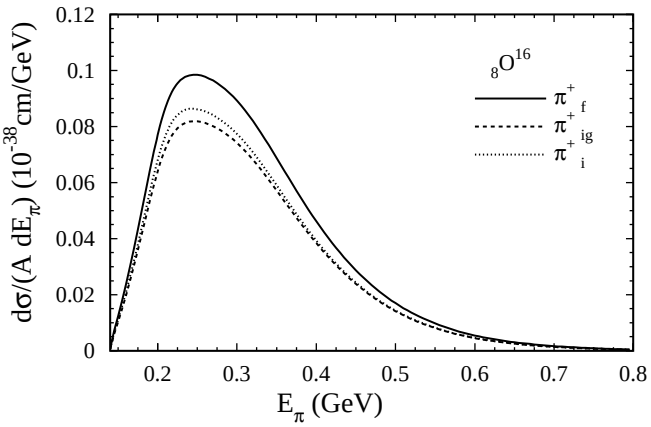

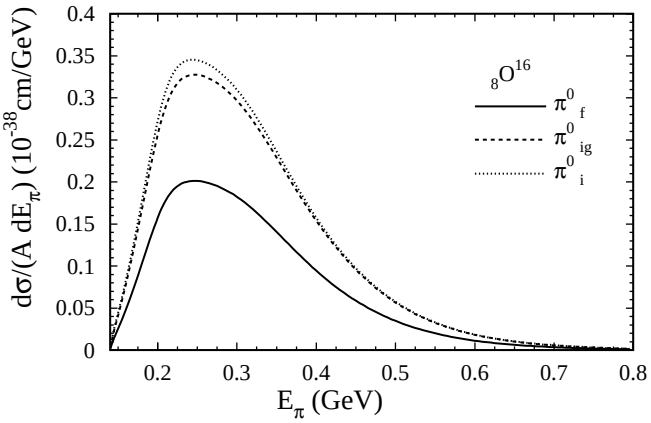

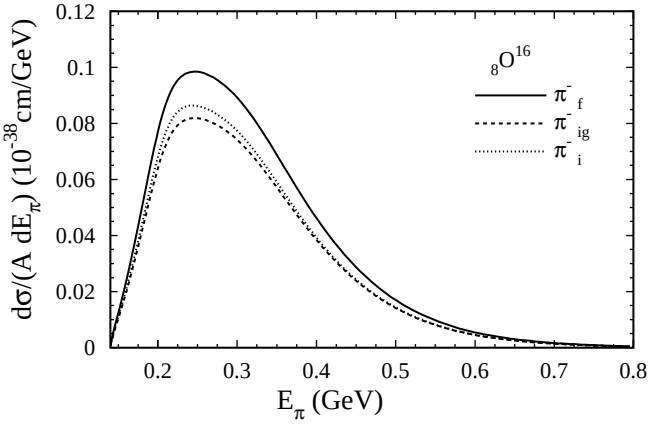

Figure 1: Differential cross section per nucleon for single pion spectra of π^+, π^0, π^- for oxygen with $E_\nu = 1$ GeV in dependence of pion energy E_π. The curves correspond to neutral current reactions.

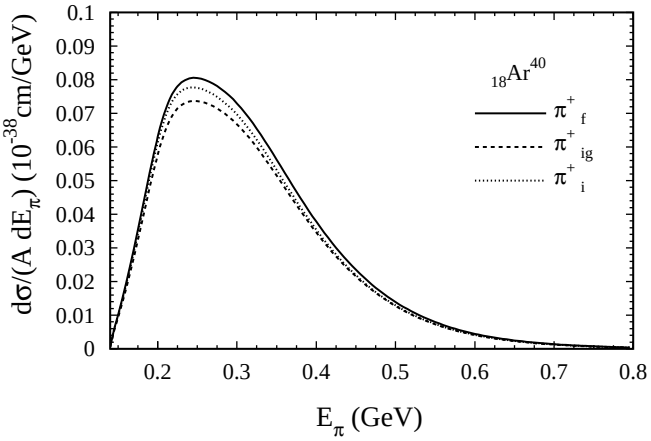

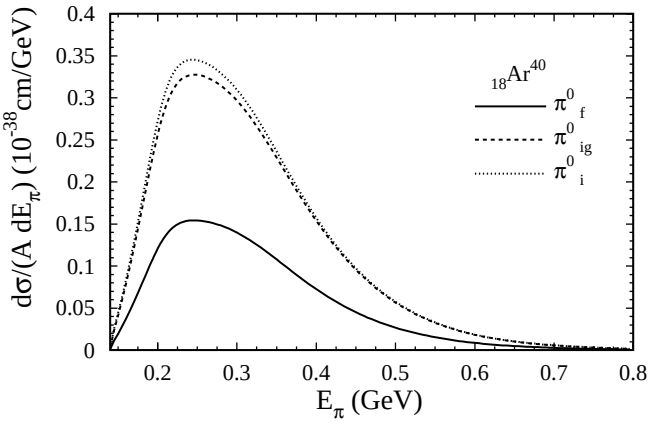

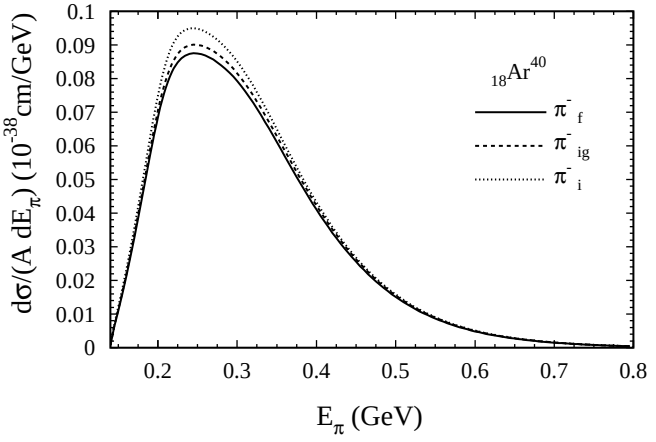

Figure 2: The same as in fig. 1 for argon.

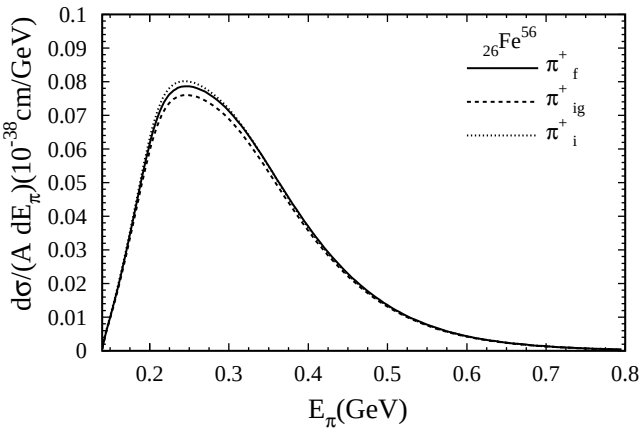

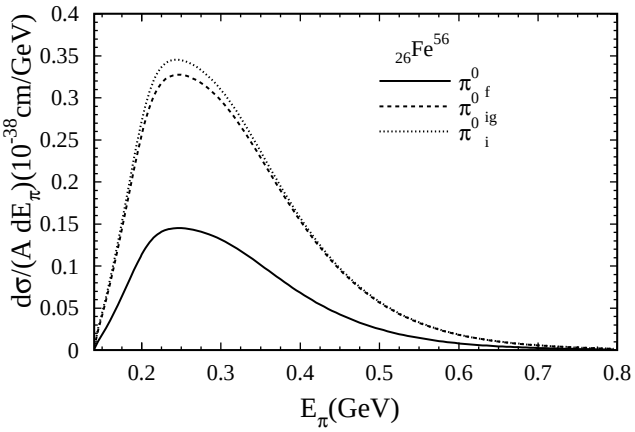

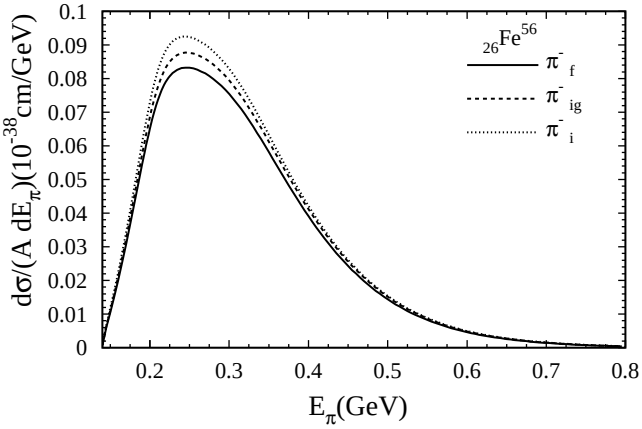

Figure 3: The same as in fig. 1 for iron.

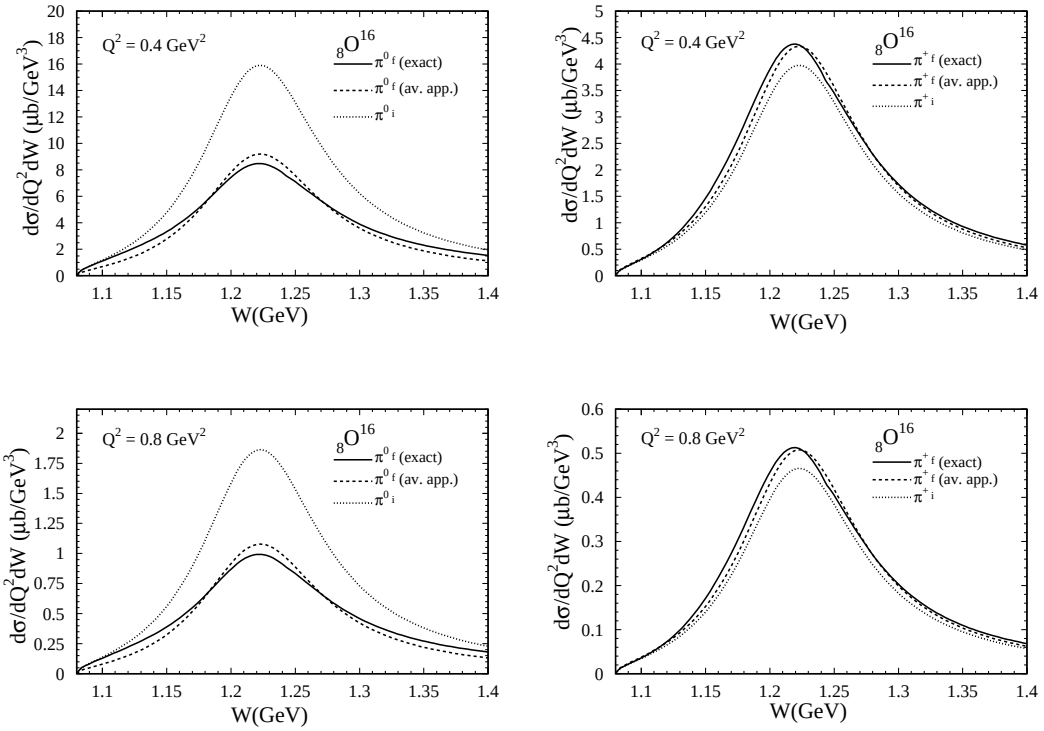

Figure 4: Double differential cross sections for single-pion electroproduction for an oxygen target in dependence of W. Spectra for π^0 and π^+ production are shown for $Q^2 = 0.4\ \mathrm{GeV}^2$ and $Q^2 = 0.8\ \mathrm{GeV}^2$ using an electron energy $E_e = 2.7\ \mathrm{GeV}$. The solid and dotted lines have been obtained according to (3.2) using the exact ANP matrix $M(W, Q^2)$ and (3.6) utilizing the double-averaged ANP matrix $\overline{\overline{M}}$ in (3.7), respectively. The dashed lines show the free nucleon cross section (3.3).

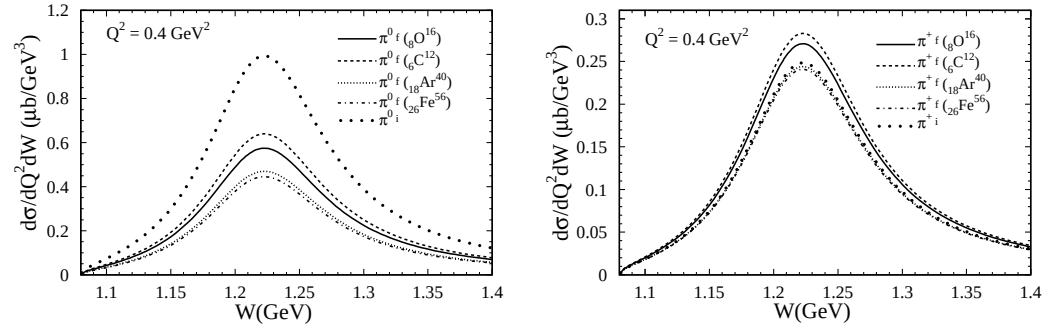

Figure 5: Double differential cross sections per nucleon for single-pion electroproduction for different target materials. W-spectra for π^0 and π^+ production are shown for $Q^2 = 0.4\ \mathrm{GeV}^2$ using an electron energy $E_e = 2.7\ \mathrm{GeV}$. The pion rescattering corrections have been calculated in the double-averaging approximation (3.6) using the ANP matrices in (3.7) and App. A. For comparison, the free nucleon cross section (3.3) is shown.

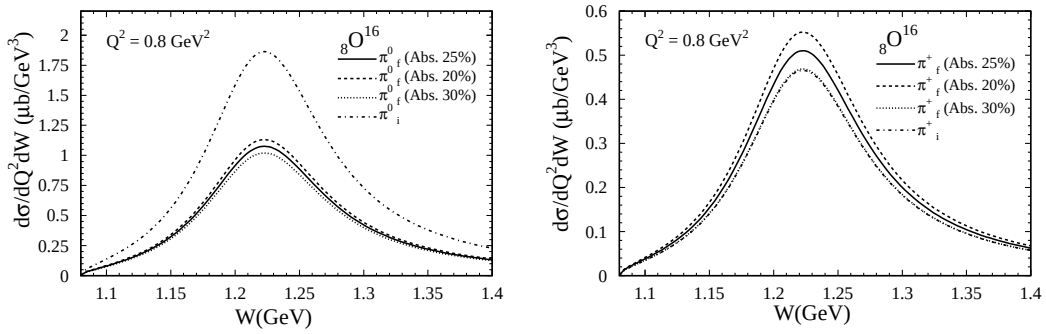

Figure 6: Double differential cross sections per nucleon for single-pion electroproduction for oxygen with 20% (dashed line), 25% (solid line) and 30% (dotted line) pion absorption. Furthermore, $Q^2 = 0.8\ \mathrm{GeV}^2$ and $E_e = 2.7\ \mathrm{GeV}$. The π^0 and π^+ spectra have been calculated in the double-averaging approximation (3.6) utilizing the matrices in App. B. For comparison, the free nucleon cross section (3.3) is shown as well.

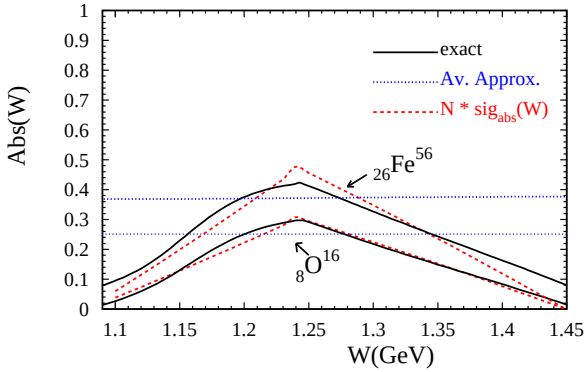

Figure 7: The fraction of absorbed pions, $\mathrm{Abs(Q^2, W)}$, in dependence of W for oxygen and iron targets for $Q^2 = 0.3\ \mathrm{GeV}^2$. Also shown is the cross section $\sigma_{\mathrm{abs}}(W)$ (model B) multiplied by free normalization factors (dashed lines). The dotted lines are the result for $\mathrm{Abs(Q^2, W)}$ in the averaging approximation.

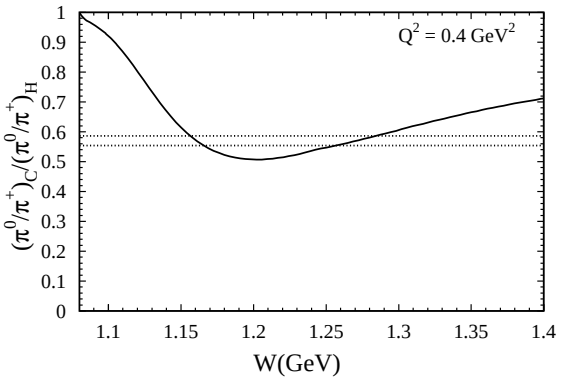

Figure 8: Double ratio of single pion electroproduction cross sections in dependence of W for fixed $Q^2 = 0.4$ GeV^2 as defined in Eq. (3.10). The dotted lines show results in the double averaging approximation with varying amounts of absorption.